INSTITUTE OF PHYSICS PUBLISHING NANOTECHNOLOGY
Nanotechnology **17** (2006) 1843–1850 doi:10.1088/0957-4484/17/8/006

Photoconductivity in single wall carbon nanotube sheets

Shaoxin Lu and Balaji Panchapakesan

Delaware MEMS and Nanotechnology Laboratory, Department of Electrical and Computer Engineering, University of Delaware, Newark, DE 19716, USA

E-mail: baloo@ece.udel.edu

Received 17 October 2005, in final form 24 January 2006
Published 15 March 2006
Online at stacks.iop.org/Nano/17/1843

Abstract
In this paper we report for the first time, the photoconductivity of large area sheets of single wall carbon nanotube upon laser illumination. The photoconductivity exhibited an increase, decrease or even 'negative' values when the laser spot was on different positions between contact electrodes, showing a 'position' dependent effect of photoconductivity. Photon induced charge carrier generation in single wall carbon nanotubes and subsequent charge separation across the metal–carbon nanotube contacts is believed to cause the photoconductivity changes. A net photovoltage of ∼10 mV and a photocurrent of ∼1.6 mA were produced under the laser intensity of ∼160 mW with a quantum efficiency of ∼1.5% in vacuum. The effect of the contact area between the electrodes and nanotubes, ambient pressure, laser intensity and light pulse frequency on the photoconductivity is discussed.

1. Introduction

Single wall carbon nanotubes (SWNTs) are unique nanomaterials with remarkable optical properties. In recent years, many studies have been performed on the optical properties of SWNTs to fulfil their promising applications in optics and optoelectronics. Specifically, nonlinear optical properties [1, 2], optical limiting behaviour [3], Raman scattering [4], photoluminescence [5], electroluminescence [6], photon induced molecular desorption [7], radioactive properties [8] and the photon adsorption properties [4] of SWNTs have been intensively studied. Many prototype devices and possible applications, such as ultra fast optical switching [9], nanotube antennas [10], large area transparent electrodes [11], photo detectors [12] and solar cells [12] have been proposed. While much of these research works have placed emphasis on nano-size devices, there has been a growing trend for SWNTs merging into micro and macro scale devices to provide more practical applications, as the synthesis cost of SWNTs are expected to decrease [13]. Nanotubes are not only optoelectronic materials, they also have excellent mechanical properties. Studies on large area sheets of carbon nanotubes may provide us opportunities for constructing smart structures with multiple functionalities. For example, in the fields of flat and flexible display, photo detection and flexible solar cells capable of covering non-flat surfaces, the application of macro scale multi-functional carbon nanotube ensembles is essential.

Photoconductivity of carbon nanotubes has been studied both in nano and micro scale samples. However studies on photoconductivity on macro-scale nanotube samples have not been done. In past studies, single carbon nanotube with two contact electrodes, in the form of a nanotube transistor, was employed to study the photoconductivity of single nanotube or small bundles [14–16]. A photocurrent due to photon induced electron–hole pair generation and subsequent charge separation by an electrical field was found flowing through the sample upon light illumination. In these nano devices, the possible effect of metal electrodes on the photoconductivity either through the molecular photodesorption of metals [14] or through the modulation of the Schottky barrier height [17] was mentioned. However, there was no detailed investigation of the effect of electrodes on photoconductivity. Other groups used micro scale thin nanotube films to examine photoconductivity [18, 19], which was explained as a result of gas molecule desorption from carbon nanotubes. Oxygen molecules have a doping effect on carbon nanotubes [20, 21] and change the nanotubes from intrinsic to a p-type semiconductor. If the doping level modulation induced by molecular photodesorption occurs, the conductivity and thus the resistance of the sample would also change accordingly. However, there is still disagreement whether oxygen adsorption/desorption happens at the electrodes or on nanotubes. Questions still remain as to whether the photoconductivity is due to the doping level

modulation by gas molecules, or due to the energy conversion mechanism which brings about the charge carriers generation and subsequent separation. Since all of the samples under testing have electrodes in contact with the nanotubes, are electrodes playing a part in the measured photoconductivity response?

In this paper, we report the photoconductivity of macro scale carbon nanotube sheets. These macroscopic sheets consist of millions of interconnected nanotubes bonded together by van der Waals forces. Using a relatively large sample (millimetres), the electrodes were separated far enough for us to study the effect of metal electrodes on the photoconductivity separately without interrupting each other. We found a strong charge separation at the interfaces between the electrodes and carbon nanotubes, which was neglected in previous studies due to the small sample size used. This charge separation resulted in strong photoconductivity responses in the samples. The effect of the contact area between electrodes and nanotubes, and the effect of light intensity, ambient pressure and frequency of light pulses on the photoconductivity are addressed.

2. Experimental details

Commercially obtained SWNTs were dispersed in iso-propyl alcohol and agitated for 20 h to make a uniform nanotube suspension with a concentration of $\sim$0.1 mg ml^{-1}. The SWNT suspension was then vacuum filtered through a poly (tetrafluoroethylene) filter. The resulting SWNT sheet on the filter was rinsed with iso-propyl alcohol, dried and was then peeled off the filter with a final thickness of $\sim$15 μm and a bulk density of $\sim$0.3 g cm^{-3}. The nanotube sheets produced in this way had a sheet resistivity of $\sim$0.5 to 5 $\Omega/\square$. The nanotube sheet was then cut into long strips of $\sim$2 mm $\times$ 20 mm in size. Platinum electrodes were fabricated using conventional lithography, metal deposition and lift off processes on glass slides because of its transparency for easier experimental set up. Experiments done on silicon dioxide wafer also gave very similar results. To transfer the nanotube sheet onto the electrodes [11], it was first rinsed with iso-propyl alcohol, and then directly placed on top of the electrodes. After the solution had dried, the nanotube sheets attached to the surface of the electrodes and substrate by van der Waals forces and resulted in an intimate contact between the electrodes and nanotubes. An additional electroplating step was used for some samples to increase the electrode–carbon nanotube contact areas. Dihydrogen hexachloroplatinate ($H_2PtCl_6{\cdot}6H_2O$), purchased from Alfa Aesar, was used to make a 5 mg ml^{-1} solution in DI water. The nanotube sheets were then covered by adhesive tape on both sides, which acted as a mask for electroplating, with only the portion for electroplating exposed (the parts of the nanotube sheet which would be on top of the electrodes). The nanotube sample was placed into the solution with a constant DC current of $\sim$35 mA passing through the sample. By controlling the time of electroplating, the coverage of platinum on the carbon nanotubes was controlled. The sample was then rinsed with DI water and transferred to acetone to remove the adhesive tape, followed by further sample cleaning in acetone, iso-propyl alcohol and DI water. Then the sample was transferred to an electrode pattern with

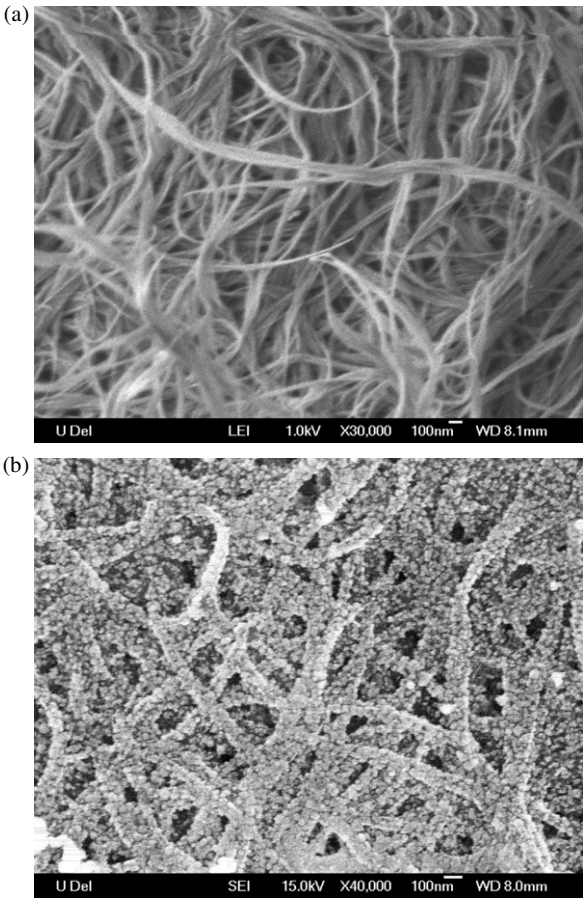

Figure 1. (a) SEM image of a SWNT sheet made by vacuum filtration. (b) SEM image of a SWNT sheet after platinum electroplating.

electroplated nanotubes sitting on top of the metal. An 808 nm semiconductor laser, which was collimated to a rectangular light spot of $\sim$1 mm $\times$ 2 mm, was used as the light source. The light intensity was recorded using a Newport 1815-C intensity meter. An Agilent 4156C semiconductor parameter analyser was used for the current and voltage measurements, because of its short response time (smaller than 1 ms) and accuracy in current measurement (better than 1 nA).

3. Result and discussion

3.1. 'Position' effect of photoconductivity

Figure 1(a) is the SEM image of the SWNT sheet composed of highly entangled SWNT bundles. Figure 2(a) schematically shows the sample with the nanotube sheet of $\sim$2 mm $\times$ 20 mm on top of the platinum electrodes, which were 1 mm in width and 10 mm apart from each other. From the top view of the sample in figure 2, an alphabetic sequence from A to E shows the five different testing positions that the laser spot would illuminate. The shaded area in the figure indicates that the laser spot of $\sim$1 mm $\times$ 2 mm was on position C, which was the centre of the sample. Positions B and D were positive and negative electrodes, respectively, while position A and E were 1 mm away from the outer edge of the electrodes. Laser

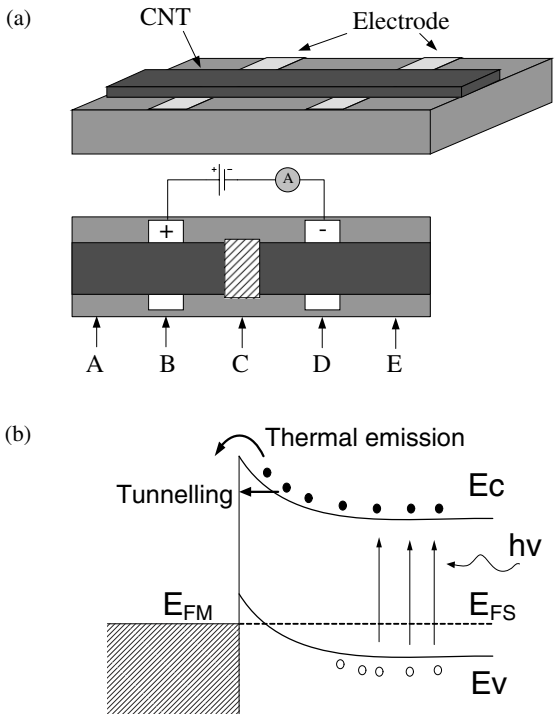

Figure 2. (a) Schematic drawing of the carbon nanotube sheets under testing. The bottom shows the top view of the device. A to E are the five testing positions on the sample where a laser spot was pointed. The shaded area indicates that the laser spot was on position C. (b) Band diagram of carbon nanotubes (right) in contact with platinum electrodes (left).

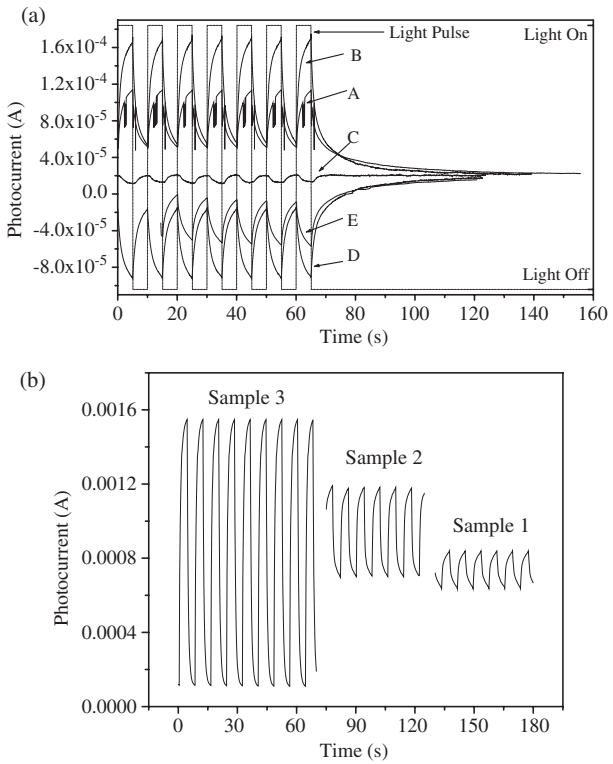

Figure 3. (a) The photocurrent of carbon nanotube sheets when the laser spot was on different positions (from A to E) of the sample. (b) Photocurrent of nanotube sheets with and without metal electroplating. Sample 1: without electroplating; sample 2: with electroplating for 5 min; sample 3: with electroplating for 20 min. The measurements were done in ∼1 mTorr vacuum.

pulses of 0.1 Hz with 50% duty cycle and 80 mW intensity was illuminated normally to the sample surface. A small voltage of 100 μV was applied to the sample during the measurement to ensure that the background current of ∼22 μA was small enough to eliminate the effect of Joule heating [19]. Rather than similar responses that would normally be expected, the photocurrent of the sample exhibited different responses when the light spot was on different positions as shown in figure 3(a).

When the laser spot was directed on the nanotubes on top of positive electrodes (position B), a dramatic increase in photocurrent from a dark value of 22 μA to ∼175 μA was observed (an increase of ∼8 times). However, when the laser spot was directed at the nanotubes on top of the negative electrodes (position D), there was a dramatic decrease in photocurrent from the dark value to ~ -90 μA, which indicated that this current overcame the original dark current, changed signs, and flowed in the 'reverse' direction, although the voltage was still forward biased. A similar effect was found in the measurement of the displacement current in a nanotube/dielectric/electrode capacitor [22], where the displacement current could be positive even when the sample was negatively biased. The built-in potential causing this effect was suspected to be the dipole layer formation or the working function difference at the interfaces. However this effect was not investigated in detail. This 'position effect' of the photocurrent showed that the positive electrode had the effect of increasing the forward current, whereas the negative electrode had the effect of increasing the backward current. Therefore, a built-in potential exists between the electrode and the nanotubes under light illumination, which would push the electrons into the electrodes, while leaving holes in the carbon nanotubes. In previous studies on micro-sized nanotube films [18, 19], this 'position effect' of the photoconductivity responses was not reported, and the effect of the electrodes on photoconductivity was also neglected. Compared to the size of the light beam, the electrodes may not be separated far enough to allow their separate investigations due to the small sample sizes. More surprisingly, when laser light was illuminated on position A and E, which was beyond the range of two metal electrodes, the changes of photocurrent similar to that of position B and D respectively, were still observed, although the amplitude of the changes were smaller. When the laser spot was in position C, a much smaller photocurrent change was witnessed, which was similar to either that of B or D, depending on which point was nearer. Repeating all of the above experiments with a halogen lamp of 120 mW cm^{-2} intensity as the white light source resulted in similar responses. However, if the whole nanotube sample was illuminated, then the change of photocurrent (increase) was quite small with only a few per cent of dark current. These results indicate that there were light induced built-in potentials at both electrodes which were opposite and competing with each other in determining the sample current.

In previous studies, the photoconductivity of nanotube films was explained as molecule desorption from the carbon nanotubes [7, 19]. The changes of conductivity $\Delta\sigma$

due to doping level modulation induced by molecular photodesorption could be expressed as:

$$\Delta\sigma = \Delta nq\mu_n + \Delta pq\mu_p \quad (1)$$

Δn and Δp are concentration changes of electrons and holes, q is the unit charge, μ_n and μ_p are charge carrier mobility. Accordingly, we would expect to see the same photocurrent response at position B, C and D and no photocurrent at position A and E, because they were not a part of the circuit. However, this was obviously different from our results. The laser had a wavelength of 808 nm. When the wavelength of light increased from UV to near-infrared (IR), the photodesorption effect became less pronounced, even under high intensity [7]. This may explain why there was no apparent effect of photodesorption in our samples.

Metal–carbon nanotube contacts have been studied previously and an energy band diagram similar to that of figure 2(b) has been suggested [23, 24], which stands for the band diagram in ideal contact conditions. When the carbon nanotubes were illuminated, photon energy was absorbed by the nanotubes, resulting in generation of electron–hole pairs or excitons [18, 25, 26]. These carriers would diffuse in carbon nanotubes randomly when there was no or only small electrical field in the sample. As they approach the metal–nanotube interface, the hot electrons might have enough energy to go across the Schottky barrier via tunnelling or thermal emission and enter the metal before they recombine with holes, as shown in figure 2(b). Once they enter the metals, the probability of going back is much smaller because of the higher energy barrier in the reverse direction, thus causing charge carrier separation. However, in almost all real metal–carbon nanotube contacts, defects and surface states exist at the interfaces, which affect the actual band structure of the contacts. The upward bending of energy bands towards metal shown in figure 2(b) may not still hold in real devices. In fact, a downward bending of energy bands towards metal could even be possible, depending on the density and types of surface states [27]. If we assume a downward bending band graph at metal–nanotube contacts instead of the one in figure 2(b), photon generated electrons will be naturally in favour of entering metal without overcoming energy barriers as discussed above. Then the charge separation effect will be more pronounced. Although the ideal theoretical models that have been proposed in the past illustrate the upward bending of energy bands, a downward bending band diagram may be more in agreement with our experimental results. Therefore, further experiments are needed to reveal the actual energy band structure of metal–carbon nanotube contacts to give a more reliable explanation of the origin of position dependent photoconductivity.

3.2. The effect of contact area on photoconductivity

For the samples discussed above, the contact area between the electrode and nanotubes was limited to be smaller than the electrode area underneath the nanotube sheet, as the contact was only made at the surface of the nanotube sheet. Upon light exposure, photo carriers diffused randomly in the sheet and may recombine to relax energy before they are separated by the electrodes. Thus, the electrode at the bottom surface of the nanotube sheet may not be effective enough to accumulate the electrons before they recombined with holes. To increase the contact areas, an additional electroplating step was done to the nanotube sheet prior to transferring to the electrode surface. Figure 1(b) shows a SEM image of the nanotubes sheet after electroplating. Compared to figure 1(a), the nanotubes were covered by a continuous layer of platinum, where the interconnected metal networks penetrated into the interconnected nanotubes networks, intimately contacted the nanotubes within the sheet and greatly increased the contact area between the nanotubes and the electrodes. To study the effect of contact area on photoconductivity, samples with different electroplating times were prepared. Figure 3(b) compares the amplitudes of the photocurrent for three samples. Sample 1: without electroplating; sample 2: electroplating for 5 min; and sample 3: electroplating for 20 min. The testing conditions of the three samples were kept the same, and the laser spot was always on the negative electrodes to ensure the comparability of results. The measurement was done in 1 mTorr vacuum. The effect of vacuum will be discussed in later sections. Compared to sample 1, sample 2 and 3 witnessed ~2 and ~8 times increases in photocurrent respectively, which clearly showed that the electroplating greatly increased the responses of photocurrent. The increases were not due to the changes of contact resistance, as the two-probe dark resistance which consists of the minor contact resistance from two metal contacts and the major intrinsic resistance of carbon nanotube sheet changed very little after the electroplating; far from enough to explain the increase of photocurrent. Rather, we believe that it was due to the increase of the contact area between the electrodes and the nanotubes. In the electroplated samples, there was more accessible electrode area for the photo carriers to approach before recombination, increasing the chances of charge separation and in turn the photocurrent. In sample 2, the coverage of platinum on the nanotubes was less than that of sample 3 due to the shorter electroplating time, which resulted in a smaller photocurrent than the later one. However, if the electroplating time was more than 20 min, the photocurrent response would not increase further due to the excess coverage of nanotubes by metal so that light could not be adsorbed by nanotubes efficiently.

3.3. Dynamic response of photoconductivity

To study the dynamic response of photoconductivity, sample 3 was used for further experiments due to its high photocurrent response. The measurements were done in 1 mTorr vacuum. By varying the laser intensity on the negative electrode of sample 3, the amplitude of the photocurrent as a function of laser intensity was recorded in figure 4, which shows a linear dependence between these two parameters. The dynamic response of the photocurrent was also measured when laser pulses of 10 mHz with a 50% duty cycle were used to excite the sample. Figures 5(a) and (b) shows the corresponding photocurrent increase with respect to the laser light and subsequent photocurrent drop without laser light, respectively. In both curves, the experimental data fit well into the exponential form of:

$$I = I_0 + A_1 \exp\left(-\frac{t}{t_1}\right). \quad (2)$$

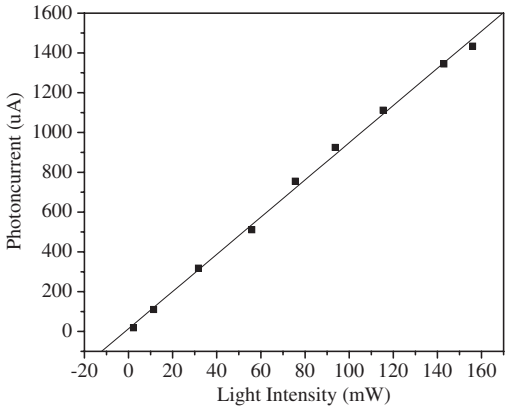

Figure 4. The amplitudes of photocurrent as a function of laser intensity. The measurements were done in ∼1 mTorr vacuum.

The time constants in equation (2) were ∼1.2 s and 1.6 s respectively, as shown in figures 5(a) and (b). To analyse them using a dynamic model, we started from the continuity equation for minority carriers [19, 26]:

$$\frac{\mathrm{d}\Delta n}{\mathrm{d}t} = -\mu_n E \frac{\mathrm{d}\Delta n}{\mathrm{d}x} + D_n \frac{\mathrm{d}^2\Delta n}{\mathrm{d}x^2} - \frac{\Delta n}{\tau} + G. \qquad (3)$$

In equation (3), Δn was the non-equilibrium minority carrier concentration; D_n was the diffusion coefficient; τ was the life time of electrons; G was the generation rate of non-equilibrium charge carriers and E was the electrical field. By assuming that the carriers were uniformly distributed in the carbon nanotubes and neglecting the electrical field, equation (4) was derived:

$$\frac{\mathrm{d}\Delta n}{\mathrm{d}t} = -\frac{\Delta n}{\tau} + \eta I \qquad (4)$$

G was substituted with ηI; η was the quantum efficiency and I was the light intensity. In steady state, $\mathrm{d}\Delta n/\mathrm{d}t = 0$ so that $\Delta n = \tau\eta I$. Assuming that the concentration of non-equilibrium carriers was proportional to the photocurrent, then the steady state photocurrent was a linear function of laser intensity, which was in agreement with our experimental results as shown in figure 4. In non-steady state, the above equation was solved to get:

$$\Delta n = \tau\eta I \left(1 - \exp\left(-\frac{t}{\tau}\right)\right) \qquad (5)$$

$$\Delta n = \tau\eta I \exp\left(-\frac{t}{\tau}\right). \qquad (6)$$

Equation (5) was for the photocurrent increase in the presence of light and equation (6) was for the photocurrent drop in the absence of light, both of which coincide with the experimental data shown in figures 5(a) and (b). The life time of electrons was of the order of 1 s, which was shorter than in [19]. While τ was attributed to photodesorption of gas molecules from the nanotubes in previous studies, the results here are interpreted as mainly due to electrode annihilation of charge carrier pairs, based on the fact that the electrode greatly affects the photocurrent.

When sample 3 was measured by varying the light pulse frequency from 50 mHz, 250 mHz, 1 Hz, 5 Hz to 20 Hz, with

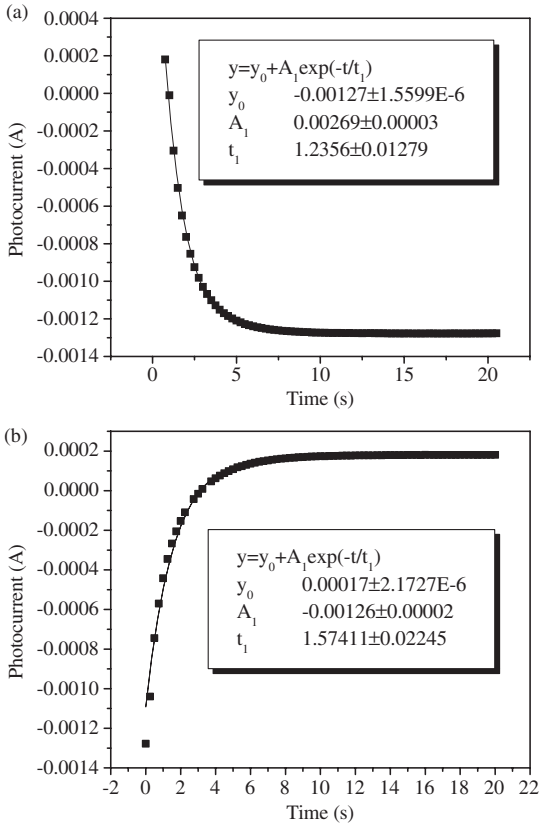

Figure 5. Typical dynamic responses ((a) laser on; (b) laser off) of photocurrent as a function of time when the laser spot was on negative electrode. The solid lines are the exponential fittings of the corresponding data. The measurements were done in ∼1 mTorr vacuum.

the laser intensity kept at 140 mW, the sample exhibited a rapid decrease in photocurrent amplitude with respect to the increase in pulse frequency, as is shown in figures 6(a) and (b). A photocurrent of ∼6 μA was still seen when the laser frequency was increased to 200 Hz. Although this current value was small, it had a much shorter response time than needed for molecular photodesorption, which was in the range of ∼10 s [7, 14, 21]. However, the question still remains as to why there was such a long time constant τ accompanying the photocurrent, as the electrodes annihilation and charge carrier recombination are normally fast processes, with a response time smaller than micro seconds [18, 22, 28].

3.4. The effect of ambient pressure on photoconductivity

We further measured the photocurrent of sample 3 by varying the ambient pressure, while the laser spot was still on the negative electrode. When a laser pulse of 125 mHz was applied to the nanotube sample, surprisingly, the amplitude of the photocurrent exhibited a dramatic increase of ∼6 times during rough pumping by a mechanical pump, as shown in figure 7(a). The inset clearly shows the increase in the photocurrent. Upon venting air into the vacuum system, the response of the photocurrent immediately went back to its previous value before pumping. In order to remove the oxygen in the vacuum system to remove its effect, the pumping-argon venting cycles

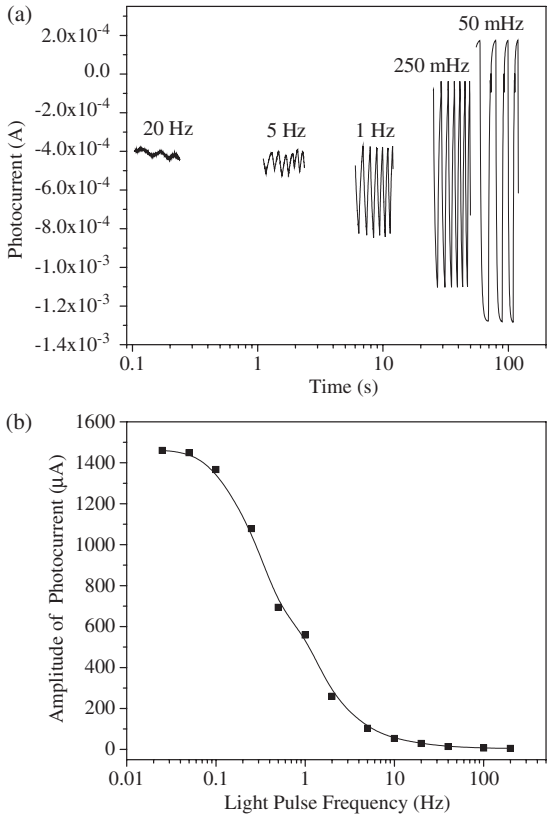

Figure 6. The frequency response of the photocurrent. (a) The photocurrent of nanotube sheets when laser pulses of different frequencies were illuminating the samples. (b) Photocurrent as a function of laser pulse frequencies. The measurements were done in ∼1 mTorr vacuum.

were repeated for more than 10 times, where similar results were repeated as in figure 7(a). A similar photocurrent response was still preserved when long time pumping of more than 100 h with vacuum better than 10^{-6} Torr to degas the sample. When the laser light was kept constant instead of using laser pulses, the photocurrent followed a similar trend of increase during pumping as shown in figure 7(b). When the photocurrent was plotted as a function of pressure, a monotone dependence was shown in the inset of figure 7(b) down to the pressure of $\sim 10^{-6}$ Torr. This dependence of photocurrent on the ambient pressure was quite stable and robust, which provide us with a novel potential application of carbon nanotubes for pressure measurement. With appropriate design and improvement in the fabrication processes of the device, the manufacture of a low cost miniature vacuum gauge with carbon nanotubes is very promising.

3.5. Opto-thermal effect of carbon nanotubes

In the absence of gas molecules, the response of the photocurrent still existed and had even higher amplitude than in the presence of gas molecules, which showed that the photocurrent of the sample was not due to the molecular desorption on nanotubes. Instead, gas molecules inhibited the photocurrent response. When gas molecules bind onto nanotube surfaces, they may act as a recombination centre or carrier traps to facilitate electron–hole pair recombination [7, 21] before they are separated by the electrodes, which may be a possible reason for this inhibiting effect. Other than the slow effect of molecule photodesorption, it was possible that the slow photocurrent response in carbon nanotubes was limited by another relative slow effect: the heating of carbon nanotubes upon light absorption. Carbon nanotubes exhibit excellent optical and thermal properties. It was shown that fluffy SWNTs could burn when exposed to a camera flash [29]. In the presence of oxygen, nanotubes burn at temperatures around 600 °C, which suggests that they absorbed significant amounts of photon energy and the local temperature of nanotubes could reach such a high point for oxidation to occur. This temperature rise, generated by multi phonon processes, involves the non-illuminative recombination of photo pumped electron–hole pairs [4]. Under higher temperature, more photon generated electrons become 'hot' electrons with higher kinetic energy, which means they have a greater probability of crossing the metal–carbon nanotube contacts, resulting in a higher photocurrent [26]. Thus, it is possible that the photocurrent was caused by charge separation of photo-generated electron–hole pairs at the metal–nanotube contacts, but limited by the relatively slow processes of sample heating by light absorption. At high ambient pressures, the sample heating by light absorption was not as much as that in high vacuum because of the good heat dissipation to the ambient. This resulted in a smaller photocurrent response than in vacuum. The slow photocurrent response may also be due to the charge trapping effect of photo carriers, which may happen on the metal/carbon nanotube contact interfaces, the contact interface between the metallic and semiconducting nanotubes and the interbundle or intertube barriers within the carbon nanotube networks. These trapped charges may take a long time to release themselves into the electrical paths. At higher vacuum, this charge trapping effect may become more apparent with less gas molecules acting as the charge recombination centres, and in turn increase the photocurrent response.

3.6. V–I characteristics

As the photocurrent response involves an energy conversion mechanism, a potential application for this technology would be the development of solar cells and photo detectors. Using sample 3, we measured the V–I characteristics of the sample under a constant light intensity of 157 mW directed at the negative electrode in a vacuum. Figure 8 shows the V–I curve with the short circuit photocurrent of ∼1.6 mA and the open circuit photovoltage of ∼10 mV, which resulted in a quantum efficiency of ∼1.5%. Theoretical work showed that carbon nanotubes could have a quantum efficiency of larger than 10% [16, 17], which indicated that there was still much room for improving this efficiency. As the separation of semiconducting nanotubes from metallic ones has become more practical in recent years [30, 31], one can use better nanotube samples with a higher proportion of semiconducting nanotubes to increase the device efficiency. In current samples, metallic carbon nanotubes have large energy band gaps due to M11 transitions between van Hove singularities, and they are much larger than that of semiconducting nanotubes, which

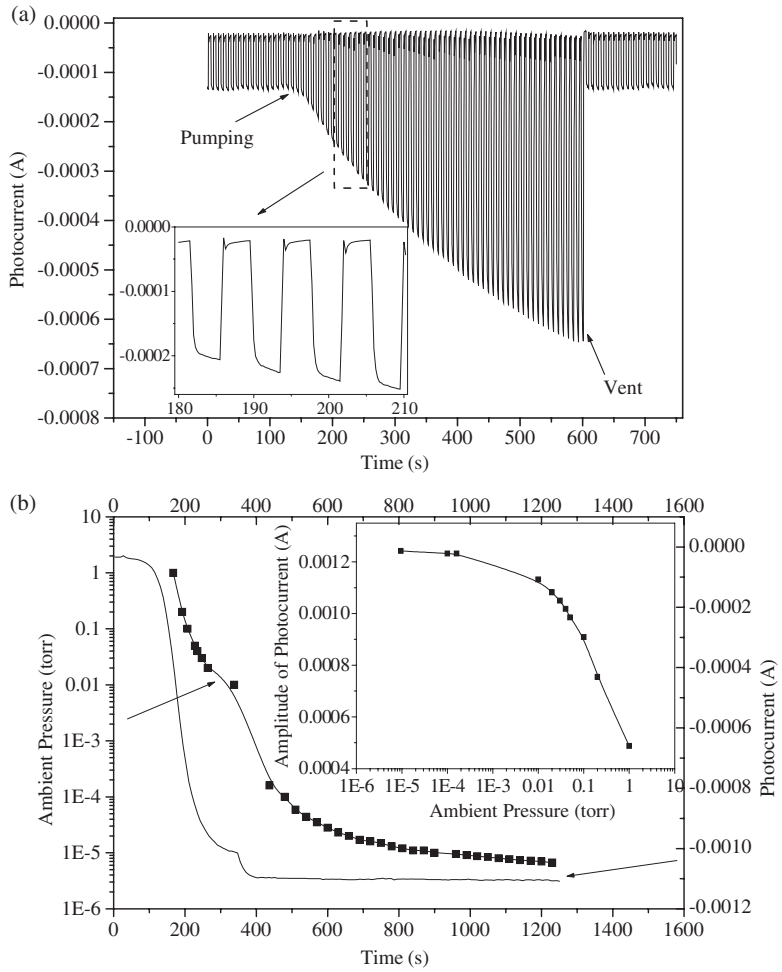

Figure 7. The effect of ambient pressure on the photocurrent of nanotube sheets. (a) *In situ* photocurrent measurement of the nanotube sheets during a pumping-venting cycle. Light pulses of 0.125 Hz with a 50% duty cycle illuminating the negative electrode of the sample. The inset is the amplified part of the indicated area to clearly show the photocurrent increases. (b) *In situ* photocurrent measurement of the nanotube sheets during pumping. Constant laser light illuminating the negative electrode of the sample. The inset shows the photocurrent as a function of ambient pressure.

correspond to S11 or S22 transitions between van Hove singularities [22, 32]. So, metallic nanotubes can only absorb near infrared light to cause intraband transitions instead of the interband transitions required for electron–hole pair generation. The use of oriented nanotubes instead of randomly oriented ones [13, 33] was also an approach to increase the efficiency, due to the anisotropic light absorption nature of carbon nanotubes [34].

4. Conclusion

The photoconductivity of large area SWNT sheets upon laser illumination is reported. The photoconductivity exhibited a 'position' dependent effect depending on the relative positions of the laser spot on the sample. Photon induced charge carrier generation in nanotubes and subsequent charge separation between the metal electrodes and the nanotubes was believed to cause these photoconductivity changes, which was limited by a relative slow sample heating effect. Larger contact areas between the electrode and the nanotubes resulted in better electron accumulation and a larger photocurrent. Higher vacuum also produced larger photocurrent. A net photovoltage of ∼10 mV and a net photocurrent of ∼1.6 mA were produced

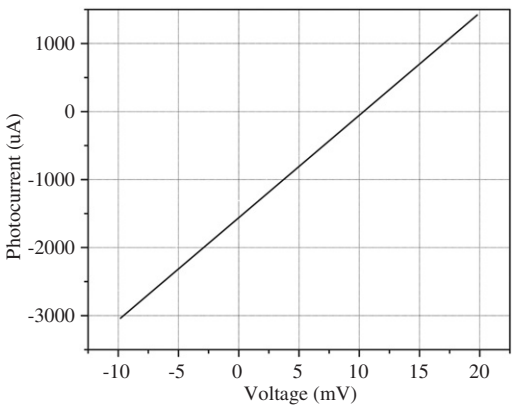

Figure 8. V–I characteristics of a carbon nanotube sheet when laser light of 157 mW was illuminating the negative electrode in a vacuum.

under a laser intensity of ∼160 mW with a quantum efficiency of ∼1.5% in a vacuum. The excellent optical properties of carbon nanotubes may find possible applications in the fields of flexible displays, photo detectors and solar cells.

Acknowledgment

Funding for this research was partially supported by the National Science Foundation Grant CCR: 0304218

References

[1] Xuchun L *et al* 1999 *Appl. Phys. Lett.* **74** 164
[2] Lauret J S, Voisin C, Cassabois G, Tignon J, Delalande C, Ph R, Jost O and Capes L 2004 *Appl. Phys. Lett.* **85** 3572
[3] Chen P, Wu X, Sun X, Lin J, Ji W and Tan K L 1999 *Phys. Rev. Lett.* **82** 2548
[4] Dresselhaus M S, Dresselhaus G and Avouris P 2001 *Carbon Nanotubes Synthesis, Structure, Properties, and Applications* (Berlin: Springer)
[5] O'Connell M J *et al* 2002 *Science* **297** 593
[6] Misewich J A, Martel R, Avouris P, Tsang J C, Heinze S and Tersoff J 2003 *Science* **300** 783
[7] Robert J C, Nathan R F, Jing K, Jien C, Thomas W T, Yuegang Z and Hongjie D 2001 *Appl. Phys. Lett.* **79** 2258
[8] Wadhawan A, Garrett D and Perez J M 2003 *Appl. Phys. Lett.* **83** 2683
[9] Hippler H, Unterreiner A-N, Yang J-P, Lebedkin S and Kappes M M 2004 *Phys. Chem. Chem. Phys.* **6** 2387
[10] Wang Y *et al* 2004 *Appl. Phys. Lett.* **85** 2607
[11] Wu Z *et al* 2004 *Science* **305** 1273
[12] Lehman J H, Engtrakul C, Gennett T and Dillon A C 2005 *Appl. Opt.* **44** 483
[13] Hata K, Futaba D N, Mizuno K, Namai T, Yumura M and Iijima S 2004 *Science* **306** 1362
[14] Moonsub S and Giles P S 2003 *Appl. Phys. Lett.* **83** 3564
[15] Kannan B, Yuwei F, Marko B, Klaus K, Marcel F, Uli W and Alf M 2004 *Appl. Phys. Lett.* **84** 2400
[16] Stewart D A and Léonard F 2005 *Nano Lett.* **5** 219
[17] Freitag M, Martin Y, Misewich J A, Martel R and Avouris P 2003 *Nano Lett.* **3** 1067
[18] Fujiwara A, Matsuoka Y, Suematsu H, Ogawa N, Miyano K, Kataura H, Maniwa Y, Suzuki S and Achiba Y 2001 *Japan. J. Appl. Phys.* **40** L1229
[19] Levitsky I A and Euler W B 2003 *Appl. Phys. Lett.* **83** 1857
[20] Collins P G, Bradley K, Ishigami M and Zettl A 2000 *Science* **287** 1801
[21] Kong J, Franklin N R, Zhou C, Chapline M G, Peng S, Cho K and Dai H 2000 *Science* **287** 622
[22] Mohite A, Chakraborty S, Gopinath P, Sumanasekera G U and Alphenaar B W 2005 *Appl. Phys. Lett.* **86** 061114
[23] Tans S J, Verschueren A R M and Dekker C 1998 *Nature* **393** 49
[24] Heinze S, Tersoff J, Martel R, Derycke V, Appenzeller J and Avouris P 2002 *Phys. Rev. Lett.* **89** 106801
[25] Korovyanko O J, Sheng C X, Vardeny Z V, Dalton A B and Baughman R H 2004 *Phys. Rev. Lett.* **92** 017403
[26] Muller R S, Kamins T I and Chan M 2002 *Device Electronics for Integrated Circuits* (New York: Wiley)
[27] Sze S M 1981 *Physics of Semiconductor Devices* (New York: Wiley–Interscience)
[28] Bunning J C, Donovan K J and Scott K 2004 *J. Appl. Phys.* **96** 3939
[29] Ajayan P M, Terrones M, de la Guardia A, Huc V, Grobert N, Wei B Q, Lezec H, Ramanath G and Ebbesen T W 2002 *Science* **296** 705
[30] Krupke R, Hennrich F, Lohneysen H v and Kappes M M 2003 *Science* **301** 344
[31] Chen Z, Du X, Du M-H, Rancken C D, Cheng H-P and Rinzler A G 2003 *Nano Lett.* **3** 1245
[32] Kataura H, Kumazawa Y, Maniwa Y, Umezu I, Suzuki S, Ohtsuka Y and Achiba Y 1999 *Synth. Met.* **103** 2555
[33] Hedberg J, Dong L and Jiao J 2005 *Appl. Phys. Lett.* **86** 143111
[34] Ichida M, Mizuno S, Kataura H, Achiba Y and Nakamura A 2004 *Appl. Phys.* A **78** 1117